machines

MDPI

Article

Trajectory Tracking of a Wall-Climbing Cutting Robot Based on Kinematic and PID Joint Optimization

Xiaoguang Liu [1,2], Zhenmin Wang [1,*], Jing Wu [3], Hongmin Wu [2] and Hao Zhang [2]

[1] School of Mechanical and Automotive Engineering, South China University of Technology, Guangzhou 510641, China; ediu_liu@163.com
[2] Key Laboratory of Modern Control Technology, Institute of Intelligent Manufacturing, Guangdong Academy of Sciences, Guangzhou 510070, China; hm.wu@giim.ac.cn (H.W.); h.zhang@giim.ac.cn (H.Z.)
[3] School of Intelligent Manufacturing, Guangzhou City Polytechnic, Guangzhou 510405, China; wujing0323@163.com
* Correspondence: wangzhm@scut.edu.cn

Abstract: Cutting is a crucial step in the industrial production process, particularly in the manufacture of large structures. In certain spatial positions, using a mobile robot, especially a wall-climbing robot (WCR) with adsorption function, is essential for carrying cutting torches to cut large steel components. The cutting quality directly impacts the overall manufacturing quality. Therefore, effectively tracking the cutting trajectory of wall-climbing cutting robots is very important. This study proposes a controller based on a kinematic model and PID optimization. The controller is designed to manage the robot's kinematic trajectory, including the torch slider, through the kinematic modeling of the wall-climbing cutting robot (WCCR). The stability of the control law is proven using the Lyapunov function, which controls the linear and angular velocities of the WCCR and the motion speed of the cross slider. Simulations verify that the control law performs well in tracking both straight-line and circular trajectories. The impact of different control law parameters on straight-line trajectory tracking is also compared. By introducing PID optimization control, the controller's anti-interference capabilities are enhanced, addressing the issue of motion velocity fluctuation when the WCCR tracks curved trajectories. The simulation and experiment results demonstrate the effectiveness of the proposed controller.

Keywords: wall-climbing and cutting robot; trajectory tracking; kinematic model; PID control

check for updates

Academic Editor: Raul D. S. G. Campilho

Received: 31 December 2024
Revised: 2 March 2025
Accepted: 11 March 2025
Published: 12 March 2025

Citation: Liu, X.; Wang, Z.; Wu, J.; Wu, H.; Zhang, H. Trajectory Tracking of a Wall-Climbing Cutting Robot Based on Kinematic and PID Joint Optimization. *Machines* **2025**, *13*, 229. https://doi.org/10.3390/machines13030229

Copyright: © 2025 by the authors. Licensee MDPI, Basel, Switzerland. This article is an open access article distributed under the terms and conditions of the Creative Commons Attribution (CC BY) license (https://creativecommons.org/licenses/by/4.0/).

1. Introduction

As industries such as shipbuilding and petrochemical storage tank construction continue to expand, the demand for mobile robots, particularly wall-climbing robots (WCR) with surface-adhesion capabilities, for welding and cutting applications has grown significantly. Over the past few decades, various mobile robots have been widely studied for welding applications in the manufacturing of large-scale equipment. Kam. B.O. et al. [1] and Dung N.M. et al. [2] developed a small, optimized, lightweight intelligent mobile welding robot for welding grids in shipbuilding. Wang J.B. et al. [3] and Jiao X.D. et al. [4] collaboratively developed a magnetic adhesion wheeled mobile welding robot for spherical storage tanks, successfully applying it to the welding of large spherical tanks. Zhang K. et al. [5] developed a mobile welding robot with a magnetic wheel mobility mechanism and a cross-slider structure for welding ship decks. Zhang H. et al. [6] developed a trackless wheel-crawler arc welding robot to realize autonomous crawling for all-position welding without a guide rail. Wu M.H. et al. [7,8] developed a wheel–leg climbing robot for

the welding and inspection of large structural equipment, enhancing the load capacity and environmental adaptability of WCRs. Gui Z.C. et al. [9] designed a novel intelligent wall-climbing welding robot (WCWR) for large steel structure manufacturing, improving welding quality and efficiency. Zhu J.S. et al. [10] developed a master–slave composite WCR system based on grooved permanent magnets for welding pressure pipelines, achieving load sharing and enhancing the flexibility and stability of the robot. Liu X.G. et al. [11] developed a crawler-type magnetic adsorption wall-climbing robot for ship welding.

To achieve autonomous welding or cutting, mobile robots must be capable of tracking weld seams or cutting paths. The trajectory tracking control of mobile robots is crucial for extending their applications. In recent years, researchers have combined advanced technologies and theories such as PID control, backstepping control, sliding-mode control, adaptive control, model predictive control (MPC), reinforcement learning, and other advanced technologies with theories, significantly advancing mobile robot trajectory tracking technology. Jin and Tack [12] utilized the kinematic model of mobile robots and Lyapunov stability theorem to design a PID tracking controller for tracking reference trajectories. Miranda-Colorado R. [13] proposed a robust PID controller applied to wall mobile robots (WMRs) using a complete kinematic model to attain low tracking errors and a fast response. Wang S. et al. [14] proposed a novel algorithm of trajectory tracking control for mobile robots using reinforcement learning and PID. They adopted Q-learning and PID for tracking the desired trajectory of the mobile robot to improve the tracking accuracy of mobile robots. Dumitrascu et al. [15] employed the backstepping method, constructing virtual feedback variables and selecting Lyapunov functions to design a tracking controller, verified through computer simulations. Hao Y.Y. et al. [16] proposed a four-wheel drive differential steering method for trajectory tracking. They designed an integral backstepping controller and constructed a simple virtual feedback variable, simplified the controller design, and improved the response speed and precision of the system. Ye Y. h. et al. [17] proposed a stable tracking control law for autonomous welding mobile robots in shipbuilding and large spherical tank welding, proving the stability of the control law using Lyapunov functions. Vishnu et al. [18] used the Euler–Lagrange method to establish a dynamic model of a mobile robot and designed a sliding-mode tracking controller with the idea of designing a sliding-mode control law by using the approach law and the backstepping method. Ling Q. et al. [19], using a kinematic and dynamic model of a mobile welding robot, established a weld tracking error system that considered external interference, and applied a non-smooth controller based on terminal sliding mode to the mobile welding robot to realize the tracking of a straight welding path. Sun et al. [20] designed an adaptive backstepping tracking controller based on the dynamic model of mobile robots, proving system stability using Barbalat's lemma and validating the controller's ability to compensate for parameter uncertainties through computer simulations. To address the nonlinearities and multivariance in the mathematical model as well as the under-actuated characteristics of WMR, Chai B. et al. [21] developed a real-time trajectory control strategy utilizing an enhanced backstepping method. Brahim Moudoud et al. [22] researched the application of fixed-time adaptive sliding-mode control (FxT-ASMC) in WMR trajectory tracking, developing a control strategy to avoid chattering and handle disturbances with uncertain upper bounds, enhancing the convergence of system states. Based on a comprehensive mathematical model of a mobile robot, Bouaziz et al. [23] proposed four control strategies—linear state feedback control, Lyapunov control, backstepping control, and sliding-mode control—to track various types of trajectories. They also compared the performance differences of these control methods in trajectory tracking. In recent years, with the development of increasingly complex mobile robot systems such as autonomous vehicles and robot dogs, trajectory tracking control algorithms for MPC [24,25] for these

complex systems has been continuously developed and optimized, and, to a certain extent, it also promotes the trajectory tracking control of mobile robots in industrial applications.

However, robots used in welding and cutting primarily rely on seam tracking systems to follow weld seams or cutting paths. These systems use mechanical contact methods [1] or non-contact methods such as laser-CCD image sensors [3,4] and laser-PSD displacement sensors [5] to obtain positional information on the weld seam as control inputs. These sensors are integrated with computer information processors in the robot control system, forming seam tracking systems that enable the trajectory tracking of the weld seam during welding. Essentially, these methods are based on position deviation PID trajectory tracking control. For weld seams with clear characteristic information, the aforementioned PID-only trajectory tracking methods can achieve good tracking performance and meet application requirements. However, for general line trajectories in cutting applications, a single PID trajectory tracking control method may not be optimal. Therefore, based on a kinematic model analysis of a WCCR, we designed a trajectory tracking controller combining the high precision of motion control and the robustness of PID control and applied it to the cutting operations of WCRs.

Although control strategies such as SMC, MPC, and FxT-ASMC can achieve ideal tracking performance for systems with nonlinearities and external disturbances, the computational resource requirements for tracking the cutting trajectory of a wall-climbing robot are particularly demanding. For cutting applications, especially plasma arc cutting, the smoothness of the cutting speed is crucial, as it directly affects the width and roughness of the cutting kerf. Even if the wall-climbing robot can track the trajectory accurately, fluctuations in motion speed can significantly impact the topography and quality of the kerf. Therefore, real-time performance requirements for robotic plasma arc cutting are extremely stringent. In contrast, the desired position and speed of a wall-climbing robot can be accurately determined through kinematic modeling during the trajectory planning stage. When combined with the advantages of the simple PID control method—such as low computational requirements, fast response, and strong robustness—reasonable parameter adjustments can be made on resource-limited mobile platforms like wall-climbing cutting robots. This approach can compensate for system nonlinearities and external interference to a certain extent, allowing the system to quickly respond to disturbances and return to the desired trajectory.

This study is organized as follows: Section 2 discusses the kinematic model and model transformation of the system, including the WCR and the sliding platform mechanism; Section 3 presents the design of the trajectory tracking controller based on the kinematic model and PID control; Section 4 discusses the tracking results under straight and circular trajectories through simulations, demonstrating the effectiveness of the proposed method; and finally, Section 5 concludes the study.

2. Kinematic Model and Stability Analysis

The WCCR utilized in this study primarily consists of a magnetic adsorption mobile robot and cross-slide modules that support a cutting torch. Figure 1 illustrates the designed 3D model of the WCCR, where (a) the main configuration of the WCCR is shown in detail, and (b) the coordinate system of the WCCR is indicated. It is equipped with four driving magnetic wheels that propel the magnetic adsorption mobile platform, along with cross-slide modules that facilitate the movement of the cutting torch via a terminal fixture. The front and rear wheels on the same side are driven by a common motor and operate at the same speed. The cross-slide modules include an x-axis slider and a y-axis slider, which are powered by two DC motors, enabling movement along the X-axis and Y-axis. In this study,

we focus exclusively on the motion of the Y-axis slider, where the central axis of the Y-axis slider is aligned with the robot's central Y-axis.

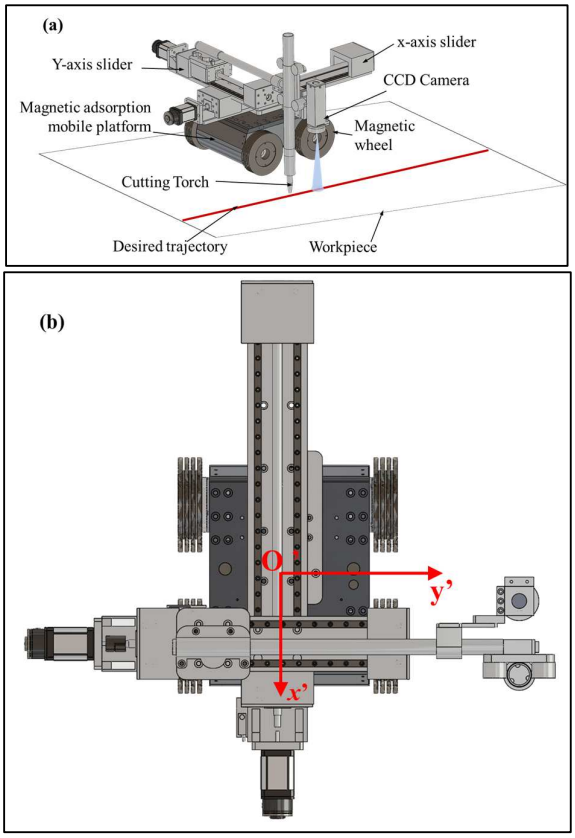

Figure 1. The 3D model of the WCCR. ((**a**) Axonometric view; (**b**) top view).

When manufacturing large-scale steel structure equipment, cutting is usually performed in a horizontal position or on a gentle slope. When a magnetic adhesion crawling robot moves on a horizontal or gently sloping surface, the friction generated by its adhesive force is sufficient to counteract the sliding tendency of the robot. Therefore, in this study, the robot's sliding is ignored, and its motion is simplified to follow a desired trajectory in a flat horizontal state. Additionally, this study considers the robot's motion model under non-holonomic constraints and makes the following assumptions:

(1) The robot operates at a relatively low speed, typically ranging from 0.3 to 0.6 m per minute or even lower, to meet the process requirements in arc welding and cutting applications;
(2) The radius of the cutting track at the non-crossing point is sufficiently larger than the robot's turning radius;
(3) The front and rear wheels on the same side of the robot maintain the same linear velocity, that is, the four-wheeled robot can be simplified into a two-wheeled robot;
(4) The center of mass and the center of rotation of the robot are coincident;
(5) The cutting torch slider moves through the robot's center, parallel to the wheel axis, and is driven by a slider motor.

To discuss the kinematic model of the WCCR, it is essential to establish a suitable coordinate system, as shown in Figure 2. In the figure, x-o-y represents the world coordinate system, while x'-o'-y' represents the robot coordinate system. The point o' is the center of the WCCR, b is the distance between the left and right wheelbase of the WCCR, r is the radius of the magnetic wheel, and l is the length of the cutting torch holder, which is controlled by torch–slide–driving motor. The variables v_L and v_R represent the linear

speeds of the left and right wheels of the robot, respectively, and v represents the forward speed of the robot. The symbol ω denotes the angular velocity of the WCCR's center.

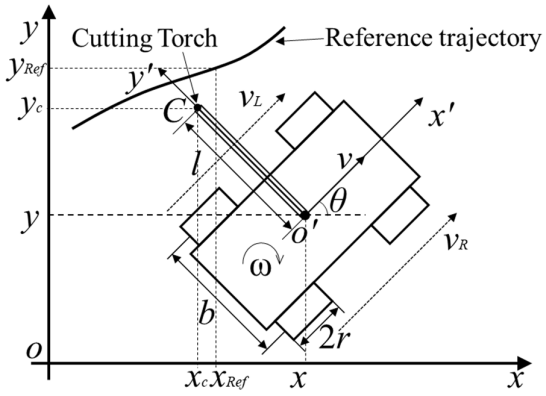

Figure 2. Kinematic model of the WCCR in a horizontal state.

The forward velocity v and angular velocity of the WCCR in its own translational coordinate system are calculated using Equations (1) and (2), as shown:

$$v = \frac{v_L + v_R}{2} \tag{1}$$

$$\omega = \frac{v_L - v_R}{b} \tag{2}$$

The position and attitude of the WCCR are represented as $q = [x\, y\, \theta]^T$, where (x, y) is the center coordinate and θ is the heading angle. The kinematics model of the WCCR is as follows [17]:

$$\begin{bmatrix} \dot{x} \\ \dot{y} \\ \dot{\theta} \end{bmatrix} = \begin{bmatrix} \cos\theta & 0 \\ \sin\theta & 0 \\ 0 & 1 \end{bmatrix} \begin{bmatrix} v \\ \omega \end{bmatrix} \tag{3}$$

The cutting torch point is set as C, where (x_c, y_c) and θ_c represent the coordinates and heading angle of the cutting point, respectively. The kinematics equation of the cutting torch point can be expressed as follows [26]:

$$\begin{cases} x_C = x - l\sin\theta \\ y_C = y + l\cos\theta \\ \theta_C = \theta \end{cases} \tag{4}$$

The derivative of (4) yields

$$\begin{bmatrix} \dot{x}_C \\ \dot{y}_C \\ \dot{\theta}_C \end{bmatrix} = \begin{bmatrix} \cos\theta & -l\cos\theta \\ \sin\theta & -l\sin\theta \\ 0 & 1 \end{bmatrix} \begin{bmatrix} v \\ \omega \end{bmatrix} + \begin{bmatrix} -\dot{l}\sin\theta \\ \dot{l}\cos\theta \\ 0 \end{bmatrix} \tag{5}$$

From Equations (3) and (5), it is evident that the control variable of the robot controller are the speed of the left wheel, the right wheel, and the horizontal cross slider. In Figure 3, the coordinates and heading angle of the point R_k on the reference trajectory are denoted by (x_{Ref}, y_{Ref}) and θ_{Ref}, respectively. Then, the kinematic differential equation of the cutting reference point Ref is as follows [17]:

$$\begin{bmatrix} \dot{x}_{Ref} \\ \dot{y}_{Ref} \\ \dot{\theta}_{Ref} \end{bmatrix} = \begin{bmatrix} \cos\theta_{Ref} & 0 \\ \sin\theta_{Ref} & 0 \\ 0 & 1 \end{bmatrix} \begin{bmatrix} v_{Ref} \\ \omega_{Ref} \end{bmatrix} \tag{6}$$

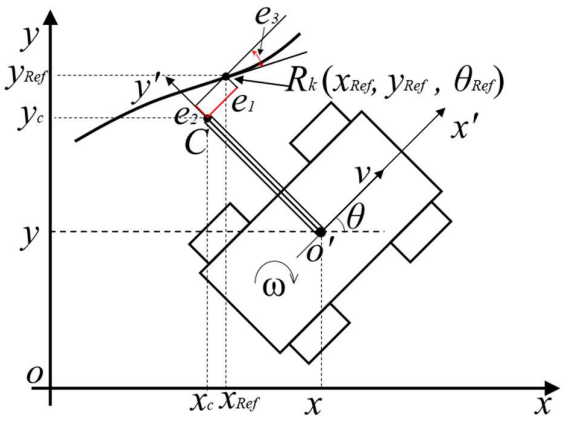

Figure 3. Trajectory deviation diagram of the WCCR.

In the global coordinate system, the tracking error of the mobile robot is defined as follows:

$$\begin{bmatrix} e_1 \\ e_2 \\ e_3 \end{bmatrix} = \begin{bmatrix} \cos\theta & \sin\theta 0 \\ -\sin\theta & \cos\theta 0 \\ 0 & 0\ \ 1 \end{bmatrix} \begin{bmatrix} x_{Ref} - x \\ y_{Ref} - y \\ \theta_{Ref} - \theta \end{bmatrix} + \begin{bmatrix} 0 \\ -l \\ 0 \end{bmatrix} \tag{7}$$

Equation (7) is expanded and differentiated, and then, Equation (4) through (6) are substituted into the result and simplified to obtain the following:

$$\begin{bmatrix} \dot{e}_1 \\ \dot{e}_2 \\ \dot{e}_3 \end{bmatrix} = \begin{bmatrix} -1 & e_2 + l \\ 0 & -e_1 \\ 0 & -1 \end{bmatrix} \begin{bmatrix} v \\ \omega \end{bmatrix} + \begin{bmatrix} v_{Ref}\cos e_3 \\ v_{Ref}\sin e_3 - \dot{l} \\ \omega_{Ref} \end{bmatrix} \tag{8}$$

Based on the preceding analysis, the trajectory tracking problem for the robot involves determining a feedback control law $\begin{bmatrix} v & \omega & \dot{l} \end{bmatrix}^T = k\left(z, z_{Ref}, v_{Ref}, \omega_{Ref}, l\right)$ under the assumption of $v_{Ref} \neq 0$ or $\omega_{Ref} \neq 0$ as $t \to +\infty$. This should ensure that $\lim_{t\to\infty}\left(z(t) - z_{Ref}(t)\right) = 0$. We define the control law of the robot, including the mobile platform and the cutting torch slider as follows [17]:

$$q_{o'} = \begin{bmatrix} v_{o'} \\ \omega_{o'} \\ \dot{l} \end{bmatrix} = \begin{bmatrix} v_{Ref}\cos e_3 + k_1 e_1 + \left[\omega_{Ref} + \frac{v_{Ref}}{2}\left(k_2(e_2 + k_3 e_3) + \frac{1}{k_3}\sin e_3\right)\right](l - k_3 e_3) \\ \omega_{Ref} + \frac{v_{Ref}}{2}\left(k_2(e_2 + k_3 e_3) + \frac{1}{k_3}\sin e_3\right) \\ k_4(e_2 + k_3 e_3) \end{bmatrix} \tag{9}$$

where k_1, k_2, k_3, k_4 are positive constants and $\dot{l}$ is the sliding velocity of the cutting torch.

According to the kinematic model of the robot, we choose the Lyapunov function, as follows [27]:

$$V = \frac{e_1^2}{2} + \frac{(e_2 + k_3 e_3)^2}{2} + \frac{1}{k_2}(1 - \cos e_3) \tag{10}$$

Furthermore, the Lyapunov function given in Equation (10) is derived and simplified. During this simplification process, Equations (8) and (9) are substituted. Additionally, we have used $\left[v, \omega, \dot{l}\right]^T = \left[v_{o'}, \omega_{o'}, \dot{l}\right]^T$. The time derivative of V is as follows:

$$\begin{aligned}
\dot{V} &= e_1\dot{e_1} + (e_2 + k_3e_3)(\dot{e_2} + k_3\dot{e_3}) + \tfrac{1}{k_2}\dot{e_3}\sin e_3 \\
&= e_1\left(v_{Ref}\cos e_3 - v + \omega l + \omega e_2\right) - (e_2 + k_3e_3)\left[\left(-\omega e_1 + v_R\sin e_3 - \dot{l}\right) + k_3\left(\omega_{Ref} - \omega\right)\right] \\
&+ \tfrac{1}{k_2}\sin e_3\left(\omega_{Ref} - \omega\right) \\
&= e_1[-k_1e_1 - \omega(l - k_3e_3) + \omega l + \omega e_2] + v_{Ref}(e_3 + k_3e_3)\sin e_3 - \omega e_1e_2 - \omega e_1k_3e_3 \\
&-k_4(e_2 + k_3e_3)^2 + \left[k_3(e_2 + k_3e_3) + \tfrac{1}{k_2}\sin e_3\right]\left(\omega_{Ref} - \omega\right) \\
&= -k_1{e_1}^2 - \omega e_1(l - k_3e_3) + \omega e_1l + \omega e_1e_2 + v_{Ref}(e_3 + k_3e_3)\sin e_3 - \omega e_1e_2 - \omega e_1k_3e_3 \\
&-k_4(e_2 + k_3e_3)^2 + \left[k_3(e_2 + k_3e_3) + \tfrac{1}{k_2}\sin e_3\right]\left(\omega_{Ref} - \omega\right) \\
&= -k_1{e_1}^2 + v_{Ref}(e_3 + k_3e_3)\sin e_3 - k_4(e_2 + k_3e_3)^2 - \tfrac{v_{Ref}k_2k_3}{2}(e_2 + k_3e_3)^2 \\
&-\tfrac{v_{Ref}}{2}(e_3 + k_3e_3)\sin e_3 - \tfrac{v_{Ref}}{2}(e_3 + k_3e_3)\sin e_3 - \tfrac{v_{Ref}}{2k_2k_3}sin^2\, e_3 \\
&= -k_1{e_1}^2 - \left(k_4 + \tfrac{v_{Ref}k_2k_3}{2}\right)(e_2 + k_3e_3)^2 - \tfrac{v_{Ref}}{2k_2k_3}(\sin e_3)^2
\end{aligned} \tag{11}$$

From Equation (10), it is definite that $V > 0$ at $[e_1,\ e_2,\ e_3]^T \neq 0$ and $V = 0$ at $[e_1,\ e_2,\ e_3]^T = 0$. Consequently, V is positive definite. From Equation (11), $\dot{V}$ is negative definite because $\dot{V} < 0$ at $[e_1,\ e_2,\ e_3]^T \neq 0$ and $\dot{V} = 0$ at $[e_1,\ e_2,\ e_3]^T = 0$. Therefore, when $e_1 = e_2 = e_3 = 0$, the system is a globally asymptotically stable equilibrium.

3. Trajectory Tracking Control Method

In this study, we utilize a PID algorithm to optimize the position and velocity of a mobile robot platform based on the kinematic controller of the robot's kinematic model. The architecture of the tracking controller for the WCCR is shown in Figure 4.

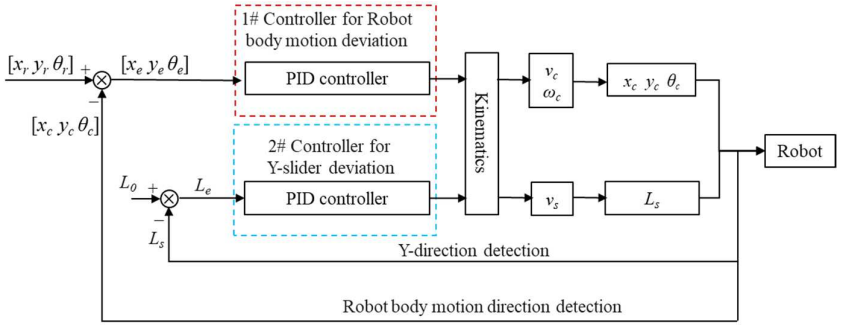

Figure 4. The structure of the proposed trajectory tracking control method. (1# indicates controller 1, 2# indicates controller 2).

The discretized PID equation is given by Equation (12):

$$\begin{aligned}
\Delta u(k) &= u(k) - u(k-1) \\
&= k_p[e(k) - e(k-1)] + k_ie(k) + k_d[e(k) - 2e(k-1) + e(k-2)]
\end{aligned} \tag{12}$$

where $u(k)$ represents the control input and $e_i(k)$ denotes the deviation at time k, with $i = 1$, 2, 3 corresponding to the robot's x-direction, y-direction, and heading angle θ, respectively. Additionally, $e_i(k-1)$ represents the deviation at the previous time step $(k-1)$.

In the process of optimizing combined with the PID controller, it is crucial to assess whether the chosen PID optimization method can maintain the stability of the WCCR system during the tracking process. This is essential for ensuring the reliability of the system's optimization design and verification. The bounded invariant ellipsoid control theory offers valuable insights in this regard. Notable contributions by researchers such as Poznyak [28,29], Khlebnikov [30], and others have advanced this field through extensive study and exploration. This study attempts to build upon these methods to demonstrate their applicability.

Given that the wall-climbing mobile robot system is inherently nonlinear, we can linearize the robot's trajectory tracking objective within a small operational range. The linearized state–space representation of the robot system can be expressed as follows:

$$\dot{x}(t) = Ax(t) + Bu(t) \tag{13}$$

where $x(t) = [x, y, \theta]^T$ represents the state vector of the robot and $u(t) = [v_L, v_R\theta]^T$ denotes the control input vector. A and B correspond to the system matrix and input matrix, respectively. Through discretization, we obtain the discrete state–space model:

$$x[k+1] = A_d x[k] + B_d u[k] \tag{14}$$

We select the Lyapunov function $V(x[k]) = x[k]^T P x[k]$, where P is a symmetric positive definite matrix, ensuring the positive definiteness of the Lyapunov function. The rate of change $\Delta V = x[k+1]^T P x[k+1] - x[k]^T P x[k]$ can be derived by substituting Equation (14) and expanding the expression:

$$\Delta V = x[k]^T A_d^T P A_d x[k] + 2x[k]^T A_d^T P B_d u[k] + u[k]^T B_d^T P B_d u[k] - x[k]^T P x[k] \tag{15}$$

Consequently, the system's bounded stability can be maintained by selecting appropriate parameters k_p, k_i, and k_d that satisfy $\Delta V < 0$. The determination of these parameters can be achieved through manual adjustment in numerical simulations, which will not be further elaborated in this study.

4. Simulation and Experiment Results

To compare the effectiveness of the optimized trajectory tracking control method, we selected two types of reference trajectories and verified the proposed control method through simulation in MATLAB R2002a (9.12.0.1884302). The trajectories and simulation parameters are designed according to the literature [17].

The first simulation uses a straight-line reference trajectory defined by x_r(t) = 0 and y_r(t) = 28. The desired velocity of the robot platform is $[v_r\ \omega_r]$ = [0.5 cm/s 0 rad/s]. The reference trajectory starts from $q_r(0) = [0\ 28\ 0]^T$, and the initial posture of the cutting torch end-effector is set as $q_c(0) = [0\ 26.5\ 0]^T$. Two sets of parameters, k_1 = 8, k_2 = 0.4, k_3 = 0.6 and k_1 = 8, k_2 = 1, k_3 = 0.4 are selected for the trajectory tracking weight control of the robot platform. Additionally, the control parameters of the cutting torch slider are chosen as k_4 = 5, k_4 = 1, and k_4 = 0.5, according to the literature. For the straight-line trajectory tracking, we directly shield the control optimization effect of the PID on trajectory tracking. The simulation results are shown in Figures 5–7. From these figures, it can be seen that the effect of tracking the straight-line trajectory is consistent with the results shown in the literature. Furthermore, the robot's speed tracking effect in Figure 7 demonstrates that the selected method and parameters exhibit a good non-oscillating performance in tracking the straight-line trajectory.

The second simulation uses a circular reference trajectory defined by x_r(t) = 1.75 × sin (0.3t) and y_r(t) = −1.75 × cos (0.3t) + 29.75. The desired velocity of the robot platform is $[v_r\ \omega_r]$ = [0.5 cm/s 0.3 rad/s]. The reference trajectory starts from q_r (0) = $[0\ 28\ 0]^T$ and moves in an anticlockwise direction. The initial posture of the cutting torch end-effector is set as q_c (0) = $[0\ 26.5\ 0]^T$. The parameter set for the WCCR is k_1 = 8, k_2 = 1, k_3 = 0.4, k_4 = 5. Figures 8 and 9 show the simulation effect without PID control.

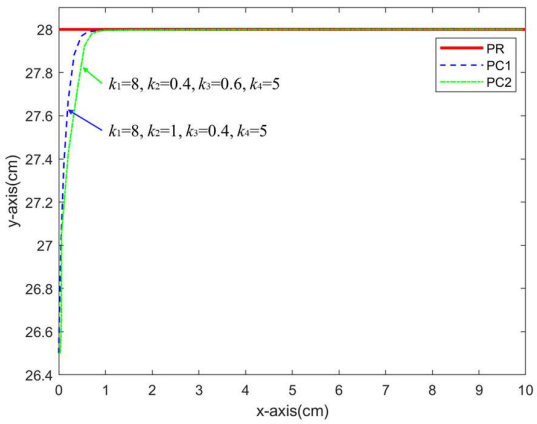

Figure 5. Straight-line tracking of the WCCR.

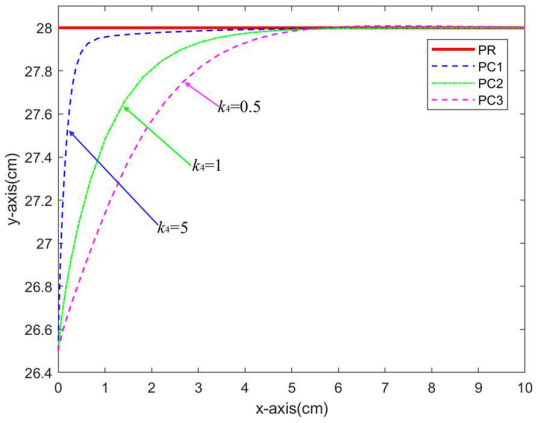

Figure 6. Straight-line tracking with different k_4 (k_1 = 8, k_2 = 1, k_3 = 0.4).

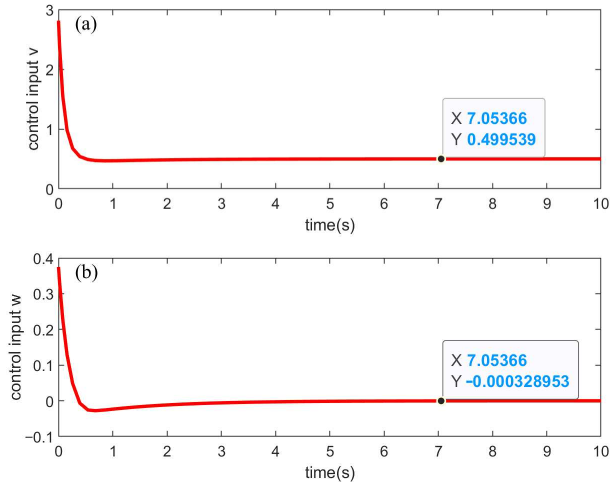

Figure 7. Robot tracking effect for a straight line on the desired velocity of $[v_r\ \omega_r]$ = [0.5 cm/s 0 rad/s]. ((**a**) represents the curve of linear velocity control quantity; (**b**) represents the curve of angular velocity control quantity).

It can be seen that for the tracking of the circular trajectory, the actual trajectory of the robot is consistent with the ideal trajectory, but the linear and angular velocities exhibit oscillations. Therefore, PID control is introduced based on kinematic control. The PID optimization control parameters are k_p = 8, k_i = 4, k_d = 0 for the speed optimization control of the WCR platform and k_p = 4, k_i = 4, k_d = 0 for the sliding platform. The simulation results are shown in Figures 10–12. These figures demonstrate that, in addition to tracking

the trajectory well, the linear and angular velocity closely approach the desired values without oscillation. Furthermore, the deviations of the actual trajectory from the desired trajectory in x, y, and θ in Figure 12 are minimal.

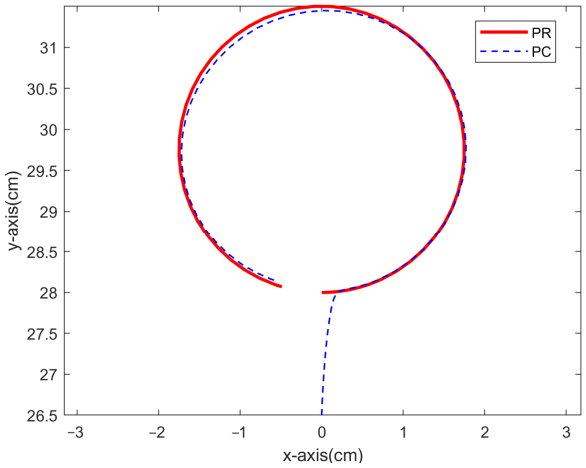

Figure 8. Circular tracking of the WCCR (k_1 = 8, k_2 = 1, k_3 = 0.4, k_4 = 5) without PID control.

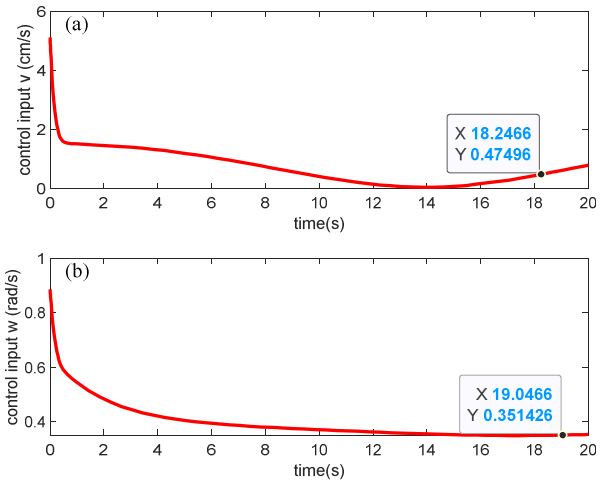

Figure 9. Robot tracking effect for a circle on the desired velocity of $[v_r\ \omega_r]$ = [0.5 cm/s 0.3 rad/s] without PID control. ((**a**) represents the curve of linear velocity control quantity; (**b**) represents the curve of angular velocity control quantity).

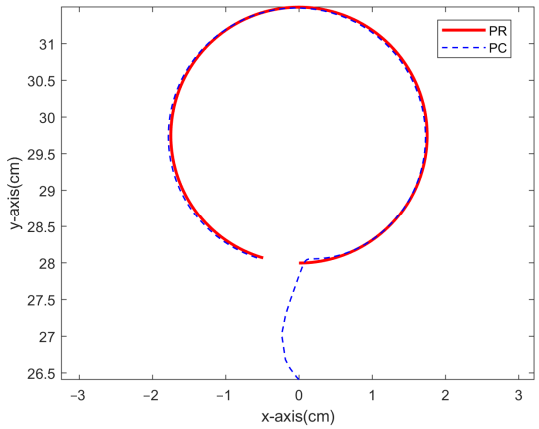

Figure 10. Circular tracking of the WCCR with the kinematic controller and PID optimization.

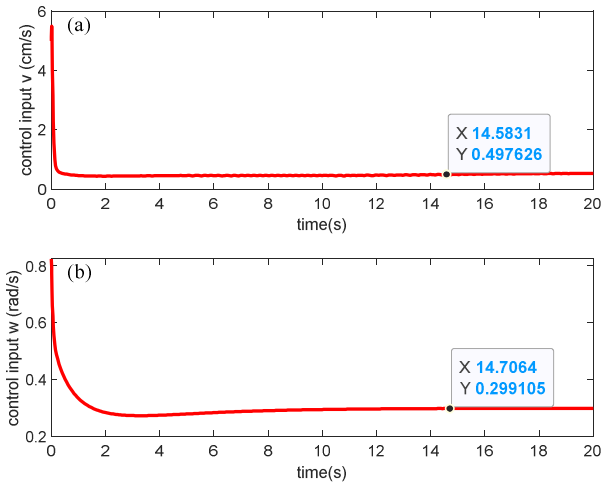

Figure 11. Robot tracking effect for a circle on the desired velocity of $[v_r\ \omega_r] = [0.5\ \mathrm{cm/s}\ 0.3\ \mathrm{rad/s}]$ with the kinematic controller and PID optimization. ((**a**) represents the curve of linear velocity control quantity; (**b**) represents the curve of angular velocity control quantity).

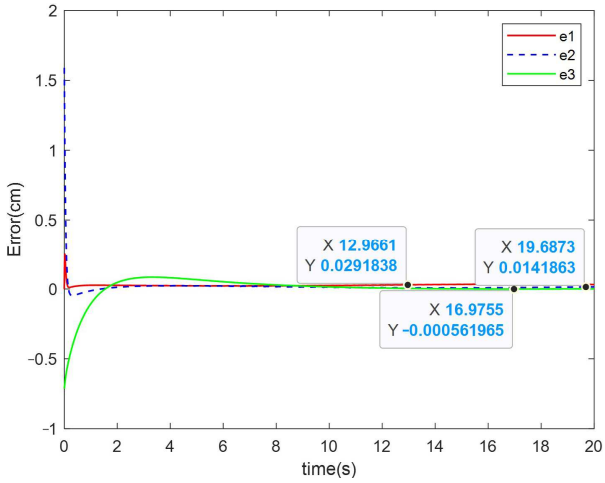

Figure 12. Deviation between the actual trajectory and desired trajectory x, y, θ with the kinematic controller and PID optimization.

The simulation results of the WCCR's trajectory tracking performance for both a straight line and a circle reveal distinct behavioral patterns. During the straight-line tracking, the system achieves satisfactory performance in terms of both trajectory accuracy and velocity stability. However, in the circular path tracking, the performance degrades, exhibiting noticeable trajectory deviations and velocity fluctuations. This phenomenon can be attributed to the kinematic control law's inherent limitations, which fail to account for the robot's steering dynamics and response time. Specifically, the WCCR must continuously adjust its heading angle and velocity during curve tracking, potentially leading to tracking lag or overshoot. Furthermore, such errors tend to accumulate over time, resulting in progressively larger deviations and reduced tracking accuracy. To mitigate errors caused by the kinematic control's slow dynamic response, the robot reduces its velocity to allow additional time for trajectory correction. However, excessively low velocities may induce oscillations and delays, further exacerbating deviations and necessitating subsequent speed increases to compensate for these errors. This cyclical behavior is clearly demonstrated in the robot's velocity profile, as shown in Figure 9. The integration of the PID control addresses these limitations by optimizing the dynamic response characteristics of the kinematic control, thereby significantly improving motion smoothness. As a result, ve-

locity fluctuations during the tracking process are markedly reduced, enhancing overall system performance.

To validate the robustness of the proposed kinematic and PID joint optimization trajectory tracking method under perturbances, we conducted simulation studies examining trajectory tracking performance under velocity step disturbances. The simulation scenario was designed with a velocity step change of 1 cm/s occurring at t = 1 s while maintaining circular trajectory tracking conditions. Comparative analyses were performed between conventional kinematic trajectory tracking control and the proposed PID-optimized approach, with particular emphasis on tracking accuracy and deviation metrics. Figures 13–15 present the velocity profiles and trajectory deviation curves of the WCCR circular path tracking under kinematic control with velocity step disturbances. In comparison, Figures 16–18 illustrate the corresponding performance metrics for the WCCR circular trajectory tracking when employing the integrated kinematic and PID optimization approach under identical perturbance conditions.

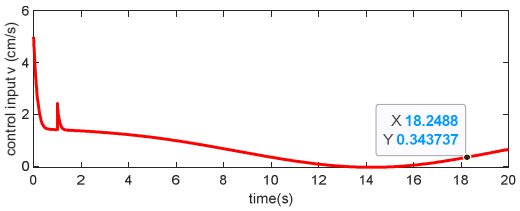

Figure 13. Velocity curve tracked under velocity step perturbance at time t = 1 s.

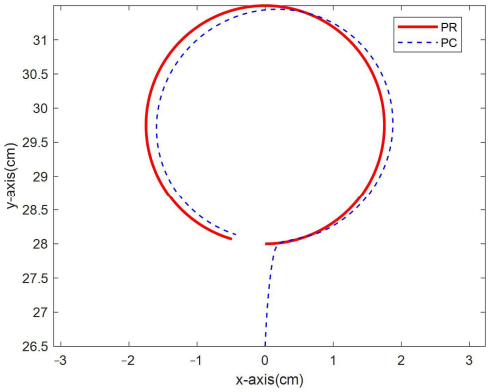

Figure 14. Compares the trajectory tracking in Figure 8 with the addition of velocity step perturbance at t = 1 s.

To more effectively demonstrate the superior tracking control performance of the WCCR's integrated kinematic and PID optimization trajectory control method compared to kinematic control under perturbance conditions, we implemented error bar representations for both x_e and θ_e deviations, thereby achieving enhanced characterization of the control performance. We observed that a step perturbance, as shown in Figure 13, was applied to the WCCR's linear velocity at t = 1 s. After the WCCR entered into the circular trajectory segment, although the actual trajectory closely followed the circular path, it deviated significantly from the desired trajectory when relying solely on the kinematic control law. Trajectory tracking in kinematic control is highly sensitive to external disturbances. In this case, a simulated linear velocity step disturbance is applied to the WCCR, resulting in an increase in the errors along the x-direction (x_e, Figure 15a), while the errors in the y-direction (y_e, Figure 15b) remain relatively stable. The angular deviation of the course (θ_e, Figure 15c) decreases progressively compared to the undisturbed scenario, ultimately causing the trajectory to shift to the right.

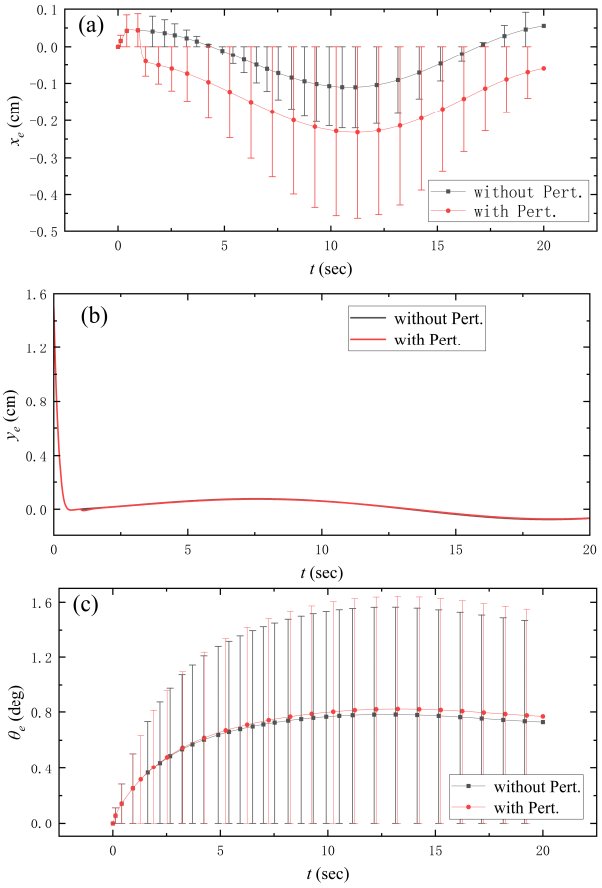

Figure 15. Comparison diagram of the WCCR circular curve tracking error without PID control. ((**a**–**c**) represent x_e, y_e, and θ_e, respectively. The black line indicates without perturbance, and the red line represents with perturbance.).

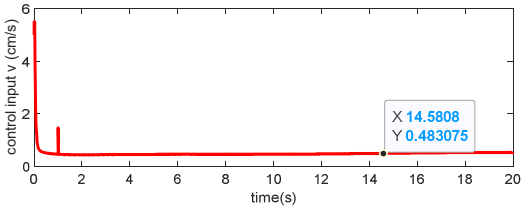

Figure 16. Velocity curve tracked under velocity step perturbance at time t = 1 s with PID control.

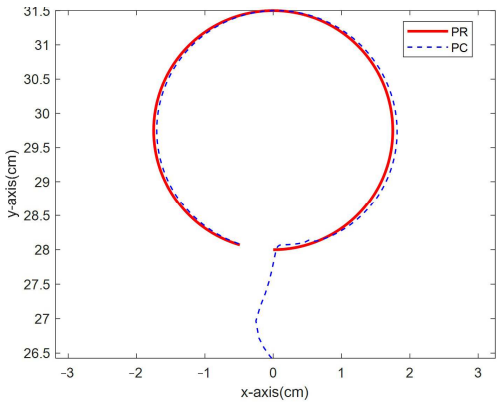

Figure 17. Compares the trajectory tracking in Figure 10 with the addition of velocity step perturbance at t = 1 s.

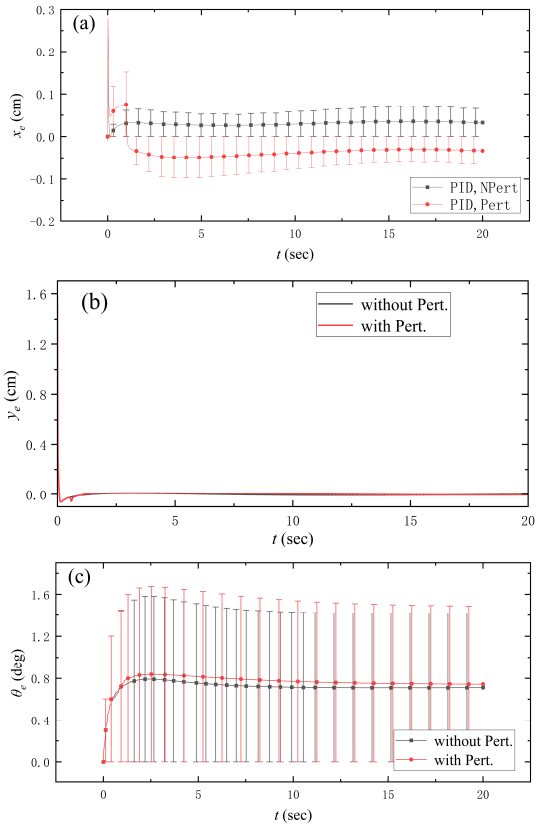

Figure 18. Comparison diagram of the WCCR circular curve tracking error optimized by combined PID control. ((**a**–**c**) represent x_e, y_e, and θ_e, respectively. The black line indicates without perturbance, and the red line represents with perturbance.).

However, when kinematic and PID joint optimization is performed, a comparison between the perturbed (Figure 16) and unperturbed conditions shows that, although there are minor variations in trajectory alignment, the x-direction error (x_e, Figure 18a) and heading angle deviation (θ_e, Figure 18c) remain stable and small in the perturbed condition compared to the undisturbed case. Ultimately, the tracking performance is significantly improved (Figure 17). This demonstrates that optimizing the PID controller enhances the kinematic controller's ability to respond to perturbances. This is attributed to the fact that the introduced PID controller dynamically adjusts the error output from the kinematic control, enabling a rapid response to system deviations. Additionally, the PID control compensates for errors and perturbances inherent in the kinematic control, thereby enhancing the robustness of the combined system against parameter uncertainties and external perturbances.

To further confirm the performance of the controller, we conducted experiments on linear and circular trajectory tracking using the WCCR, as shown in Figure 19. The results are summarized in Table 1. In the straight-line trajectory tracking test, both the pure kinematics control method and the combined kinematics–PID control method yielded similar endpoint deviations. However, in the circular trajectory tracking test, the combined kinematics–PID method demonstrated a significant improvement over the pure kinematics method.

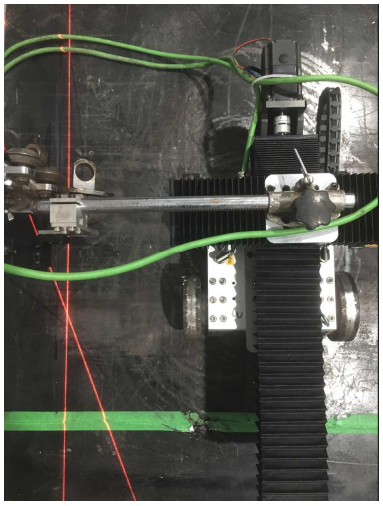

Figure 19. Trajectory tracking test platform for a wall-climbing cutting robot.

Table 1. Trajectory endpoint deviation data sheet (unit: mm).

Trajectory Type	Terminal Deviation Quantity	
	Kinematics Control	Kinematics and PID Joint Control
Straight-line trajectory tracking	1.1	1.0
Circular trajectory tracking	3.8	2.3

5. Conclusions

In this study, we propose a kinematic and PID joint optimization control method for WCCR trajectory tracking. In kinematic control law, the motion of the robot moving platform and cross slider are considered simultaneously.

The proposed kinematic trajectory tracking control law for the WCCR demonstrates effective performance in straight-line trajectory tracking. Through parameter optimization, it achieves both slight tracking errors and smooth velocity curves.

However, when applied to circular trajectory tracking, the control law exhibits velocity fluctuations. To address this limitation, a PID control method was integrated with the kinematic controller, improving the response of the WCCR to kinematic control law, resulting in a notable improvement in the stability of the robot's velocity.

To validate the robustness of the combined kinematic and PID control method against perturbances, a step perturbance was introduced to the robot's linear velocity. The simulation experimental results preliminarily confirm the method's robustness and feasibility under such disturbances.

Although the introduction of PID control in this study has optimized the trajectory tracking performance of the WCCR under kinematic control, providing a viable solution for improving its tracking accuracy, the parameter tuning process for PID remains relatively complex. Furthermore, due to space limitations, the study does not include a comprehensive experimental validation of the proposed control method. Future research will focus on enhancing the kinematic model by incorporating external dynamic factors, investigating the method's robustness against various types of disturbances, and designing a systematic experimental framework to thoroughly validate its applicability.

Author Contributions: Conceptualization, X.L. and Z.W.; methodology, X.L. and Z.W.; software, H.W. and H.Z.; validation, J.W. and X.L.; formal analysis, X.L.; investigation, X.L., H.W. and H.Z.; resources, Z.W.; data curation, X.L., H.W. and H.Z.; writing—original draft preparation, X.L.; writing—review and

editing, Z.W.; visualization, X.L.; supervision, Z.W.; project administration, J.W.; funding acquisition, Z.W. All authors have read and agreed to the published version of the manuscript.

Funding: This research was funded by the Science and Technology Project of Guangdong Province (grant no. 2021B1515420006, 2021B1515120026), the National Natural Science Foundation of China (grant no. U2141216, 51875212, 62203126), the Guangdong Basic and Applied Basic Research Foundation (2022A1515240013), the Characteristic Innovation project of colleges and universities in Guangdong Province (grant no. 2021KTSC272), GDAS' Project of Science and Technology Development (2022GDASZH-2022010108), the Marine Economy Development (Six Marine Industries) Special Fund Project of Guangdong Province (grant no. GDNRC [2021]46), and the Science and Technology Plan Project of Jiangmen City (2023780200050009211).

Data Availability Statement: The data presented in this study are available on request from the corresponding author.

Conflicts of Interest: Authors Xiaoguang Liu and Hao Zhang are employed by the Key Laboratory of Modern Control Technology, Institute of Intelligent Manufacturing, Guangdong Academy of Sciences. The remaining authors declare that the research was conducted in the absence of any commercial or financial relationships that could be construed as a potential conflict of interest.

Abbreviations

The following abbreviations are used in this manuscript:

PID	Proportional integral derivative
WCR	Wall-climbing robot
WCCR	Wall-climbing and cutting robot
CCD	Charge-coupled device
PSD	Position sensitive detector
FxT-ASMC	Fixed-time adaptive sliding-mode control
PR	Position of reference
PC	Position of cutting torch
Pert.	Perturbance

References

1. Kam, B.-O.; Jeon, Y.-B.; Kim, S.-B. Motion control of two-wheeled welding mobile robot with seam tracking sensor. In Proceedings of the 2001 IEEE International Symposium on Industrial Electronics, Pusan, Republic of Korea, 12–16 June 2001; Volume 2, pp. 851–856.
2. Dung, N.M.; Duy, V.H.; Phuong, N.T.; Kim, S.B.; Oh, M.S. Two-Wheeled Welding Mobile Robot for Tracking a Smooth Curved Welding Path Using Adaptive Sliding-Mode Control Technique. *Int. J. Control Autom. Syst.* **2007**, *5*, 283–294.
3. Wang, J.B.; Sun, Z.G.; Chen, Q.; Ji, M.; Jiang, L.P.; Jiao, X.D.; Xue, L. CCD Sensor Assisted Weld Seam Tracking Method for Spherical Tank Welding Robot. *Trans. China Weld. Inst.* **2001**, *22*, 31–34.
4. Jiao, X.D.; Xue, L.; Jiang, L.P.; Li, M.; Sun, Z.; Wang, J.; Chen, Q. Seam Tracking of a Rail—Free Spherical Tank Welding Robot Based on the Trajectory Estimation Algorithm. *China Mech. Eng.* **2003**, *14*, 187–189.
5. Zhang, K.; Lv, X.Q.; Wu, Y.X.; Zhang, Y. Mobile robot for welding ship decks with function of auto-searching weld line. *Trans. China Weld. Inst.* **2005**, *4*, 55–59.
6. Zhang, H.; Pan, J.L.; Xu, J.N.; Liu, G.P.; Liu, W.L.; Liu, Z.W.; Yan, B.Y.; Gao, L.S. Trackless Crawl Type All-position Arc Welding Robot System. *Chin. J. Mech. Eng.* **2006**, *42*, 85–91. [CrossRef]
7. Wu, M.; Pan, G.; Zhang, T.; Chen, S.; Zhuang, F.; Zhao, Y.Z. Design and Optimal Research of a Non-Contact Adjustable Magnetic Adhesion Mechanism for a Wall-Climbing Welding Robot. *Int. J. Adv. Robot. Syst.* **2013**, *10*, 63. [CrossRef]
8. Wu, M.H. Research on Wall-Climbing Robot with Wheel Leg and Non-Contact Magnetic Adhesion Mechanism for Welding Tasks. Ph.D. Thesis, Shanghai Jiao Tong University, Shanghai, China, 2014.
9. Gui, Z.C.; Deng, Y.J.; Sheng, Z.X.; Xiao, T.; Li, Y.; Zhang, F.; Dong, N.; Wu, J. Design and experimental verification of an intelligent wall-climbing welding robot system. *Ind. Robot* **2014**, *41*, 500–507. [CrossRef]
10. Zhu, J.S.; Sun, Z.G.; Huang, W.; Chen, Q. Design of a Master-Slave Composite Wall Climbing Robot System for Penstock Assembly Welding. In Proceedings of the Intelligent Robotics and Applications, ICIRA 2019, Shenyang, China, 8–11 October 2019.

11. Liu, X.G.; Zhou, Y.; Jiang, X.M.; Cao, L. Control System of a Wall Climbing Robot for Automatic Welding. In Proceedings of the 5th International Conference on Information Science and Control Engineering (ICISCE 2018), Zhengzhou, China, 20–22 July 2018.
12. Jin, T.S.; Tack, H.H. Path following control of mobile robot using Lyapunov techniques and PID controller. *Int. J. Fuzzy Log. Intell. Syst.* **2011**, *11*, 49–53. [CrossRef]
13. Miranda-Colorado, R. Observer-based proportional integral derivative control for trajectory tracking of wheeled mobile robots with kinematic disturbances. *Appl. Math. Comput.* **2022**, *432*, 127372. [CrossRef]
14. Wang, S.; Yin, X.; Li, P.; Zhang, M.; Wang, X. Trajectory Tracking Control for Mobile Robots Using Reinforcement Learning and PID. *Iran. J. Sci. Technol. Trans. Electr. Eng.* **2020**, *44*, 1059–1068. [CrossRef]
15. Dumitrascu, B.; Filipescu, A.; Minzu, V.; Filipescu, A. Backstepping control of wheeled mobile robots. In Proceedings of the 15th International Conference on System Theory, Control and Computing, Sinaia, Romania, 14–16 October 2011.
16. Hao, Y.Y.; Wang, J.; Chepinskiy, S.A.; Krasnov, A.J.; Liu, S. Backstepping based trajectory tracking control for a four-wheel mobile robot with differential-drive steering. In Proceedings of the 36th Chinese Control Conference, Dalian, China, 26–28 July 2017.
17. Ye, Y.H.; Zhang, H.; Gao, Y.F. Stable tracking control of autonomous welding mobile robots based on kinematics model. In Proceedings of the 2010 International Conference on Computer Application and System Modeling (ICCASM 2010), Taiyuan, China, 22–24 October 2010.
18. Vishnu Prasad, S.; Vinod, P.; Ajmal, M.S. Development of backstepping sliding mode tracking control for Wheeled Mobile Robot. In Proceedings of the 2014 IEEE International Conference on Advanced Communications, Control and Computing Technologies, Ramanathapuram, India, 8–10 May 2014.
19. Qiao, L.; Huang, Z.H.; Zhu, J.C. Seam Tracking for Mobile Welding Robot Based on Terminal Sliding Mode. *Procedia Manuf.* **2019**, *37*, 227–235. [CrossRef]
20. Sun, D.H.; Cui, M.Y.; Li, Y.F. Adaptive backstepping control of wheeled mobile robots with parameter uncertainties. *Control Theory Appl.* **2012**, *29*, 1198–1204.
21. Chai, B.; Zhang, K.; Tan, M.; Wang, J. An Optimal Robust Trajectory Tracking Control Strategy for the Wheeled Mobile Robot. *Int. J. Control Autom. Syst.* **2024**, *22*, 1050–1065. [CrossRef]
22. Moudoud, B.; Aissaoui, H. Fixed-time adaptive sliding mode-based trajectory tracking control for Wheeled Mobile Robot: Theoretical development and real-time implementation. *e-Prime Adv. Electr. Eng. Electron. Energy* **2024**, *10*, 100830. [CrossRef]
23. Bouaziz, N.I.; Besseghieur, K.L.; Achour, N. Trajectory Tracking Control for a Differential Drive Mobile Robot. In Proceedings of the International Conference on Electrical Engineering and Control Applications (ICEECA 2022), Khenchela, Algeria, 15–17 November 2022.
24. You, Y.L.; Yang, Z.; Zhuo, H.Z.; Sui, Y. Research on ground mobile robot trajectory tracking control based on MPC and ANFIS. *Control Eng. Pract.* **2024**, *152*, 106040. [CrossRef]
25. Chu, D.; Li, H.; Zhao, C.; Zhou, T. Trajectory tracking of autonomous vehicle based on MPC with PID feedback. *IEEE Trans. Intell. Transp. Syst.* **2023**, *24*, 2239–2250.
26. Bui, T.H.; Chung, T.L.; Nguyen, T.T.; Chung, T.L.; Kim, S.B. A simple nonlinear control of a two wheeled welding mobile robot. *Int. J. Control Autom. Syst.* **2003**, *1*, 35–42.
27. Kim, D.H.; Oh, J.H. Globally asymptotically stable tracking control of mobile robots. In Proceedings of the IEEE International Conference on Control Applications, Trieste, Italy, 1–4 September 1998.
28. Poznyak, T.; Chairez, I.; Perez, C.; Poznyak, A. Switching robust control for ozone generators using the attractive ellipsoid method. *Isa Trans.* **2014**, *53*, 1796–1806. [CrossRef]
29. Poznyak, A.; Azhmyakov, V.; Mera, M. Practical output feedback stabilization for a class of continuous-time dynamic systems under sample-data outputs. *Int. J. Control* **2011**, *84*, 1408–1416. [CrossRef]
30. Khlebnikov, M.V.; Polyak, B.T.; Kuntsevich, P.M. Optimization of linear systems subject to bounded exogenous disturbances: The invariant ellipsoid technique. *Autom. Remote Control* **2011**, *72*, 2227–2275. [CrossRef]

Disclaimer/Publisher's Note: The statements, opinions and data contained in all publications are solely those of the individual author(s) and contributor(s) and not of MDPI and/or the editor(s). MDPI and/or the editor(s) disclaim responsibility for any injury to people or property resulting from any ideas, methods, instructions or products referred to in the content.